Journal of Polish CIMAC
Gdansk University of Technology
The Faculty of Ocean Engineering and Ship Technology

AFFECT OF DECARBURISATION TIMES OF BAINITIC FERRITE LATHS ON THE MICROSTRUCTURE IN Fe-Cr-C STEEL

Zdzisław Ławrynowicz

University of Technology and Life Sciences, Mechanical Engineering Faculty
Department of Materials Science and Engineering
av. Kaliskiego 7, 85-789 Bydgoszcz, Poland, e-mail: lawry@utp.edu.pl

Abstract

The purpose of the present paper is to demonstrate how a thermodynamic method can be used for solving a problem of the decarburisation of bainite laths. The paper presents an investigation of the time required for the diffusion of carbon out of supersaturated laths of ferrite into the retained austenite. This should in principle enable to examine the partitioning of carbon from supersaturated ferrite laths into adjacent austenite and the carbon content in retained austenite using analytical method. The obtained results illustrates that the estimated times are not capable of decarburising the sheaf of ferrite included thick laths of bainitic ferrite during the period of austempering. A consequence of the precipitation of cementite from austenite during austempering is that the growth of bainitic ferrite can continue to larger extent and that the resulting microstructure is not an ausferrite but it is a mixture of bainitic ferrite, retained austenite and carbides.

Keywords: *carbon diffusion, decarburisation*

1. Introduction

The attractive properties of carbide free bainitic steel are related to its unique microstructure that consists of ferrite and high carbon austenite. Because of this microstructure, the product of austempering reaction is often referred to as “ausferrite” rather than bainite [4,6,13]. If bainite is formed by a shear mechanism it is supposed that bainitic ferrite is supersaturated with carbon and any excess carbon is soon rejected into the residual austenite. It is supposed that the decarburisation time of ferrite lath is a function of lath width and increases with decreasing temperature because the diffusion coefficient of carbon also decreases with temperature. The decarburisation time also increases as the thickness of the ferrite laths increases.

The purpose of the present paper is to demonstrate how a thermodynamic method can be used for solving a problem of the decarburisation of bainite laths and this should in principle enable to examine the possibility of carbides precipitation in Fe-0.38C-0.93Cr steel during bainite reaction.

2. Material and methods

The chemical composition of the steel is listed in Table 1. The concentration of alloying elements is obtained from the chemical analysis.

Tab. 1. Chemical composition and calculated B_S and M_S temperatures of the steel used in the present study. All concentrations are given in wt. %*

Steel	C	Si	Mn	P	S	Cr	Ni	B_S, °C	M_S, °C
Fe-0.38C-0.93Cr	0.38	0.29	0.63	0.01	0.025	0.93	0.11	505	320

*The B_S and M_S temperatures are calculated by using methods developed by Bhadeshia [4]

A high-speed Adamel Lhomargy LK-02 dilatometer was used to establish change of length ($\Delta L/L$) during isothermal bainitic transformation. In order to ensure rapid cooling (300 Ks^{-1}) from austenitising temperature, the specimens were 13mm in length and 1.1mm in diameter. The temperature was measured with a 0.1mm diameter NiCr-Ni thermocouple welded to the sample. Cooling was carried out by blowing a helium gas directly onto the surface of the sample. Determination of the linear expansion coefficients was carried out in the UBD Leitz-Wetzlar dilatometer. Thin foils for transmission electron microscopy were prepared from discs slit from heat-treated specimens. The discs were mechanically thinned to 50 μm and were electropolished until perforation occurred in a twin jet polishing unit containing an electrolyte of 5% perchloric acid, 25% glycerol and 70% ethyl alcohol mixture solution. The electrolyte temperature was maintained around – 10°C, the polishing potential was 55 V at a current of 30 mA. The foils were examined in a Tesla BS-540 transmission electron microscope operated at 120 kV.

3. Phase diagram

The phase diagram of Fe-0.38C-0.93Cr steel (Fig. 1) was calculated as in Ref. [2,3,10] using a model developed by Bhadeshia [1,16], based on the McLellan and Dunn quasi-chemical thermodynamic model [15]. The bainite B_S and martensite M_S start temperatures were also calculated using the same method [1,16]. The determined carbon concentration of residual austenite x^{γ} at the points where the formation of bainite terminate were compared against the extrapolated T_0, T_0', and A_3' phase boundaries for Fe-0.38C-0.93Cr steel. In presented diagram (Fig. 1) the reaction is found to stop when the average carbon concentration of the residual austenite is between the T_0 and T_0' lines and in some cases beyond the T_0 line (black circles in Fig. 1). Carbon concentration in retained austenite at the cessation of reaction is close to the T_0' line and supports formation of bainitic ferrite by a shear mechanism. Since diffusionless transformation is not possible beyond the T_0 curve, the obtained results need explanation. This might be explained by the fact that the T_0' line accounts for 400 J/mol of stored energy in the bainite. If this energy is reduced by plastic deformation of the surrounding austenite then a higher volume fraction of bainite should be able to form. Secondly, when carbide precipitation accompanies the development of bainitic ferrite laths as a secondary process, it reduces the carbon content in the austenite and allows the bainitic reaction to proceed to a larger extend.

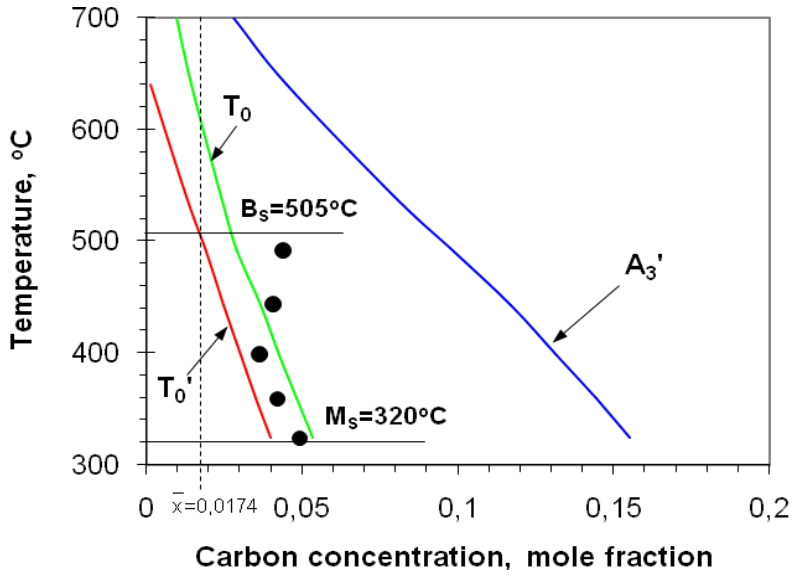

Fig. 1. The calculated phase boundaries A_3', T_0 and T_0' for the investigated Fe-0.38C-0.93Cr steel together with all the experimental data of the measured carbon contents of the untransformed austenite (black circles)

4. Microstructural analysis

Microstructure of typical upper bainite after holding the Fe-0.38C-0.93Cr steel at 480°C for 2h is seen in Fig. 2. Retained austenite films exist between the ferrite laths. Because carbides were not observed in the ferrite it means that the excess carbon in these ferrite laths partitions into the residual austenite soon after the growth event. The isolated films of austenite can accumulate carbon concentration beyond T_0' line (Fig. 1). Because the austenite is greatly enriched in carbon they cannot transform to bainite once the T_0' line is exceeded. Furthermore, these thin films of the residual austenite are stable to martensitic transformation on cooling to ambient temperature.

Fig. 3 shows microstructure obtained by isothermal transformation at 350°C for 60 seconds. Transmission electron microscopy revealed that the sheaves were composed of much smaller laths of ferrite and the microstructure contain only bainitic ferrite and carbon enriched residual austenite films. In Fig. 2 and 3 it is seen that the morphology of bainitic ferrite is lath rather than plate. Bainitic ferrite laths of thickness about 0.2÷0.3μm form separately one from another. Retained austenite was present between the ferrite laths as thin films. The ability to retain such films of austenite is due to partitioning of carbon into residual austenite following the formation of supersaturated bainitic ferrite. Carbides were not observed in ferrite laths of thickness thinner than 0.2μm. In this case films of residual austenite can accumulate all the excess carbon from supersaturated ferrite laths of thickness less than 0.2μm. It is a possibility that in the later stage of transformation, the carbon concentration of untransformed austenite is decreased by the carbide formation and then the reaction can proceed to a larger extent. The determined microstructural parameters of Fe-0.38C-0.93Cr steel after isothermal transformation are listed in Table 2.

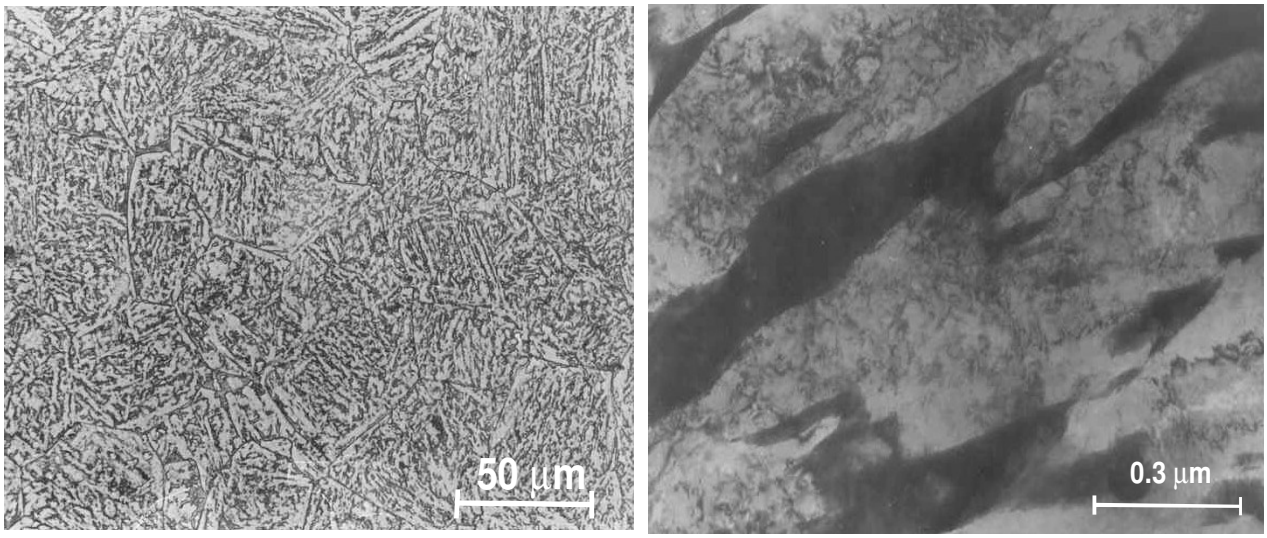

a) b)

Fig. 2. Microstructure of Fe-0.38C-0.93Cr steel after isothermal transformation at 480°C for 2h, a) light microscopy, etched with 2% nital, b) TEM, thin foil

a) b)

Fig. 3. Microstructure of Fe-0.38C-0.93Cr steel after isothermal transformation at 350°C for 60 seconds, a) light microscopy, etched with 2% nital, b) TEM, thin foil

Tab. 2. Microstructural parameters of Fe-0.38C-0.93Cr steel

Microstructural parameters	Transformation temperature, °C	
	350	480
Average austenite grain size, μm	30	30
Volume of bainite in the form of packets, %	74	41
Average packet length, μm	26	21
Average packet width, μm	17	19
Average width of bainite lath, μm	0.2	0.3
Morphology of retained austenite	thin films, also irregular islands	irregular islands and thin films

5. Method used in estimating the decarburising time of the bainitic ferrite laths

Kinsman and Aaronson [7] first considered the kinetics of the partitioning of carbon from bainitic ferrite of the same composition as the parent phase. For a plate of thickness w_α the flux of carbon is defined along a coordinate z normal to the α/γ interface, with origin at the interface and z being positive in the austenite (Fig. 4).

The method used to calculate the time of decarburising of bainitic ferrite laths is based on the hypothesis that transformation to bainite can only occur in regions of austenite where $x_\gamma \le x_{T_0}$, where x_γ is the carbon concentration in austenite and x_{T_0} is the carbon concentration corresponding to the T_0 curve. As a lath of bainitic ferrite forms it partitions its excess carbon into the retained austenite. This creates a carbon diffusion field around the lath. Another parallel lath (of the same sheaf) which forms subsequently can only approach the original lath to a point where $x_\gamma \le x_{T_0}$. The method assumes that the interval between laths formations is larger than the time required to decarburise each lath.

The time t_d needed to decarburise the ferrite is intuitively expected at least to be comparable to that required for a lath to complete its growth. If t_d is small relative to the time required to relieve the carbon supersaturation by the precipitation of carbides within the ferrite, then upper bainite is obtained, otherwise lower bainite forms [5,8,11].

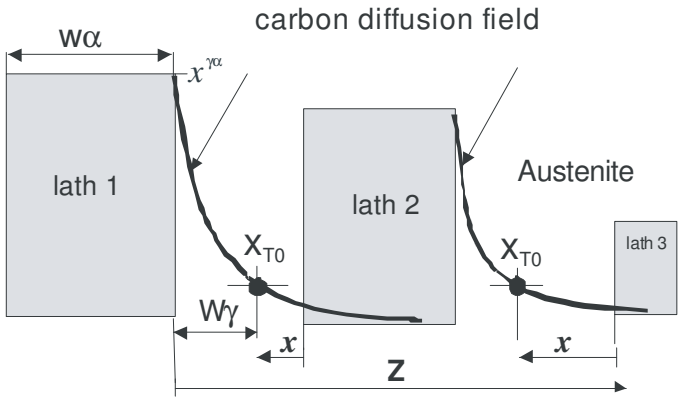

Fig. 4. Schematic diagram of method used in estimating the time of decarburising the bainitic ferrite laths. Lath 1 forms first and lath 2 and 3 and next is allowed to approach it to point where $x_\gamma \le x_{T_0}$ (distance of this point from lath 1 is denoted w_γ). This is in fact the thickness of the retained austenite film. The mean thickness of the retained austenite films is almost tenfold thinner (0.01-0.02μm) than the average thickness of the bainitic ferrite laths (~0.2μm).

6. The calculation of decarburisation times of supersaturated bainitic ferrite laths

The problem therefore becomes a calculation of the decarburisation times of all bainite laths that exist in all bainite packets inside austenite grains (Fig. 5). The time needed to decarburize the ferrite laths within bainite sheaves, t_{dz}:

$$t_{dz} = \sum_i t_{di} \tag{1}$$

where t_{di} is the time required to decarburise individual supersaturated bainitic ferrite lath of specific thickness $w_{\alpha i}$.

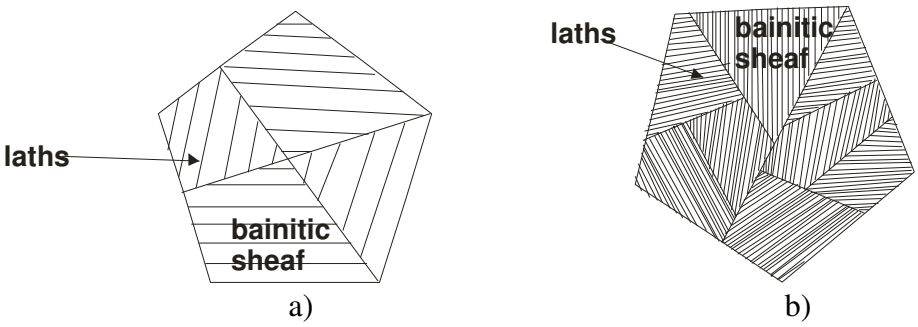

Fig. 5. Schematic illustration of bainite packets size and lath size (width) formed at higher (a) and lower (b) transformation temperature with different thickness of bainitic ferrite laths

Because of the inhomogeneous distribution of carbon and other solutes in the matrix after transformation to bainite the retained austenite is enriched to a greater extent in the immediate vicinity to bainite platelets than in the regions between the bainitic sheaves (Fig. 4, 5) while those regions contain relatively poor carbon [12,14]. Martensite is usually found to be in the blocky regions of untransformed austenite [3]. It indicates that the blocky regions of austenite between bainitic sheaves are less enriched with carbon, and therefore are thermally unstable.

From the mass balance for carbon it follows that [2]:

$$(0.5w_\alpha)(\bar{x} - x^{\alpha\gamma}) = \int_{z=0}^{\infty} [x_\gamma\{z, t_d\} - \bar{x}]dz \tag{2}$$

where $\bar{x}$ is the average mole fraction of carbon in the alloy and $x^{\alpha\gamma}$ and $x^{\gamma\alpha}$ are the paraequilibrium carbon concentration in ferrite and austenite respectively. Since the diffusion rate of carbon in austenite is slower than in ferrite the rate of decarburization will be determined by the diffusivity in the austenite and the concentration of carbon in austenite at the interface remains constant for times $0 < t < t_d$ after which it steadily decreases as the austenite becomes homogeneous in composition. The function x_γ is given by:

$$x_\gamma = \bar{x} + (x^{\gamma\alpha} - \bar{x})erfc\{z / 2(Dt_d)^{0.5}\} \tag{3}$$

This assumes that for $t < t_d$, the concentration of carbon in the austenite at the interface is given by $x^{\gamma\alpha}$.

The diffusion coefficient of carbon in austenite $D\{x\}$, is very sensitive to the carbon concentration and this has to be taken into account in treating the large concentration gradients that develop in the austenite. It is clearly necessary to know $D\{x\}$ at least over a range $\bar{x} \to x^{\gamma\alpha}$, although experimental determinations of $D\{x\}$ do not extent beyond $x = 0.06$. The value of D was calculated as discussed in Ref. [1]. The good approximation of the dependent diffusivity of carbon in austenite can be a weighted average diffusivity $\overline{D}$ [3,15]. Taking into account carbon concentration gradients it has been demonstrated that for most purposes a weighted average diffusivity $\overline{D}$ can adequately represent the effective diffusivity of carbon [3,9]. Weighted average

diffusivity $\overline{D}$ is calculated by considering the carbon concentration profile in front of the moving ferrite interface as given by the following equation:

$$\overline{D} = \int_{\bar{x}}^{x^{\gamma\alpha}} \frac{D dx}{(x^{\gamma\alpha} - \bar{x})} \tag{4}$$

On carrying the integration, the time required to decarburise a supersaturated bainitic ferrite lath of thickness w_α is given by [2,3]:

$$t_d = \frac{w_\alpha^2 \pi (\bar{x} - x^{\alpha\gamma})^2}{16\overline{D}(x^{\gamma\alpha} - \bar{x})} \tag{5}$$

where: $\bar{x}$ is the average carbon concentration in the alloy, $x^{\alpha\gamma}$ and $x^{\gamma\alpha}$ are the carbon concentrations in ferrite and austenite respectively, when the two phases are in paraequilibrium.
The calculated diffusion coefficients of carbon in austenite and carbon concentration in austenite $x^{\gamma\alpha}$ and ferrite $x^{\alpha\gamma}$ after isothermal transformation at 350 and 480°C of Fe-0.38C-0.93Cr steel are listed in Tab. 3.

Tab. 3. The calculated diffusion coefficients of carbon in austenite $D\{x\}$ and a weighted average diffusivity $\overline{D}$ and carbon concentration in austenite $x^{\gamma\alpha}$ and ferrite $x^{\alpha\gamma}$ after austempering at 350 and 480°C of Fe-0.38C-0.93Cr steel

Diffusion coefficients	Austempering temperature, °C	
	350	480
D, m^2/s	0.1856 x 10^{-16}	0.2172 x 10^{-14}
$\overline{D}$, m^2/s	0.2462 x 10^{-15}	0.6638 x 10^{-14}
Carbon concentration, mol		
in austenite, $x^{\gamma\alpha}$	0.1310	0.0809
in ferrite, $x^{\alpha\gamma}$	0.5426 x 10^{-3}	0.6920 x 10^{-3}

Calculated decarburisation times (t_d) of distance 30 μm (average austenite grain size) consisted of laths with thickness: 0.05, 0.1, 0.2, 0.3, 0.5, 1.0, 5.0 and 10 μm in Fe-0.38C-0.93Cr steel are shown in Tab. 4.

Tab. 4. Decarburisation times (t_d) of distance 30 μm consisted of laths with thickness: 0.05, 0.1, 0.2, 0.3, 0.5, 1.0, 5.0 and 10 μm in Fe-0.38C-0.93Cr steel

T_i, °C	Decarburisation times (t_d) of distance of 30 μm in seconds							
	3x10 μm	6x5 μm	30x1 μm	60x0.5 μm	100x0.3 μm	150x0.2 μm	300x0.1 μm	600x0.05 μm
350	5202	2601	520.2	260.1	156.1	104.0	52.0	26.0
480	604.8	302.4	60.5	30.2	18.1	12.1	6.0	3.0

The calculated times of partitioning are shown in Fig. 6 for different thickness of bainitic ferrite phase (for w_o=0.1, 0.2, 0.5, 1.0, 10, 50, and 100 μm) and austempering temperatures. For investigated Fe-0.38C-0.93Cr steel calculations show that t_d increases sharply as temperature decreases.

The decarburisation time t_d is a function of lath width and increases with decreasing temperature of isothermal transformation (480 and 350°C) because the diffusion coefficient of carbon also decreases with temperature (Table 3).

Furthermore, it is generally observed that the width of ferrite laths is highly diverse (Fig. 2 and 3) in different packets. This reflect the possibility that cementite can precipitate in thicker bainite laths (when t_d is a long period of time) and in thinner laths has not during isothermal transformation. If the decarburisation process dominates it leads to the formation of upper bainite.

It is also consistent with the fact that upper and lower bainite often form at the same temperature in a given steel or ductile iron [2,3,11]. The decarburisation time also increases as the thickness of the ferrite phase increases (Fig. 6).

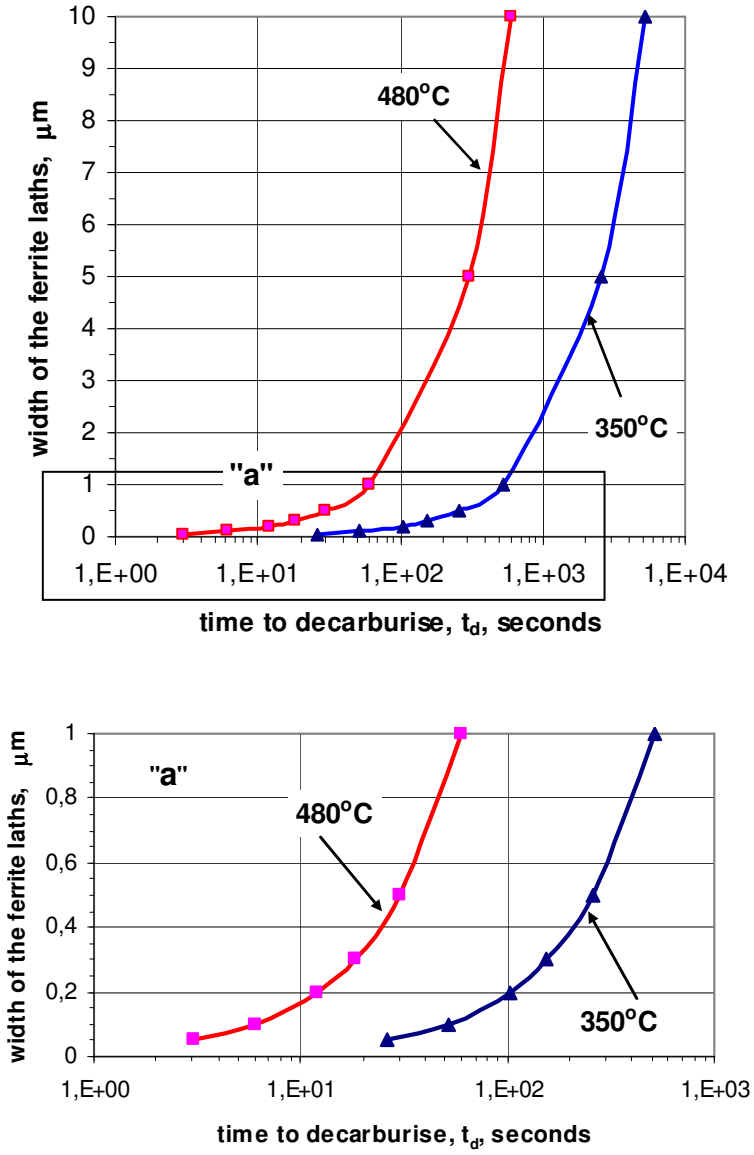

Fig. 6. The calculated decarburisation times for a given width of ferrite phase in investigated Fe-0.38C-0.93Cr steel after austempering at 480 and 350°C. The relationship (5) has been used for calculations

The obtained results illustrates that the estimated times are not capable of decarburising the sheaf of ferrite included thick laths during the period of isothermal holding. A consequence of the precipitation of cementite from austenite during austempering is that the resulting microstructure is not an ausferrite but it is a mixture of bainitic ferrite, retained austenite and carbides.

Conclusions

As a result the following conclusions are reached:

1. Analytical calculations of the time required for the diffusion of carbon out of supersaturated laths of ferrite into the retained austenite indicate that there is a necessity of carbides precipitation from ferrite or/and austenite.
2. A consequence of the precipitation of cementite from ferrite or/and austenite during austempering is that the growth of bainitic ferrite can continue to larger extent and that the resulting microstructure is not an ausferrite but is a mixture of bainitic ferrite, retained austenite and carbides.

References

[1] Bhadeshia, H.K.D.H., *Diffusion of carbon in austenite,* Metal Science, vol. 15, 477-479, 1981.

[2] Bhadeshia, H.K.D.H., Christian, J.W., *Bainite in Steels,* Metallurgical Transactions A, 21A, 767-797, 1990.

[3] Bhadeshia, H.K.D.H., *Bainite in Steels,* Institute of Materials, 1-458, London, 1992.

[4] Chang, L.C., *Carbon content of austenite in austempered ductile iron,* Scripta Materialia, vol. 39, No 1, 35-38, 1998.

[5] Christian, J.W., *Theory of transformations in metals and alloys,* p. 778, Oxford, Pergamon Press, 1965.

[6] Guzik, S.E., *Austempered cast iron as a modern constructional material,* Inżynieria Materiałowa, vol. 6, 677-680, 2003.

[7] Kinsman, K.R., Aaronson, H.I., *The transformation and hardenability in steels,* Climax Molybdenum Company, Ann Arbor, MI, p.39, 1967.

[8] Kutsov, A. at al., *Formation of bainite in ductile iron,* Materials Sci. and Engineering, A273-275, 480-484, 1999.

[9] Ławrynowicz, Z., *Criticism of selected methods for diffusivity estimation of carbon in austenite,* Zeszyty Naukowe ATR, nr 216, Mechanika, vol. 43, 283-287, 1998.

[10] Ławrynowicz, Z., *Mechanism of bainite transformation in Fe-Cr-Mo-V-Ti-C steel,* International Journal of Engineering, vol. 12, 81-86, 1999.

[11] Ławrynowicz, Z., *Transition from upper to lower bainite in Fe-Cr-C steel,* Materials Science and Technology, vol. 20, 1447-1454, 2004.

[12] Ławrynowicz, Z., *A discussion on the mechanism of bainite transformation in steels,* Technology and Materials,. Gdańsk, Politechnika Gdańska, vol. 4, pp. 149-155, 2006.

[13] Pietrowski, S., *Nodular cast iron of bainitic ferrite structure with austenite or bainitic structure*, Archives of Materials Science, vol. 18, No.4, 253-273, 1997.

[14] Shiflet, G.J., Hackenberg, R.E., *Partitioning and the growth of bainite,* Scripta Materialia, vol. 47, 163-167, 2002.

[15] Siller, R.H., McLelan, R.B., *The Application of First Order Mixing Statistics to the Variation of the Diffusivity of Carbon in Austenite,* Metallurgical Transactions, vol. 1, 985-988, 1970.

[16] Takahashi, M., Bhadeshia, H.K.D.H., *A Model for the Microstructure of Some Advanced Bainitic Steels,* Materials Transaction, JIM, vol. 32, 689-696, 1991.